arXiv:astro-ph/0301389v1 20 Jan 2003

The cannonball model of gamma ray bursts

Arnon Dar
Technion, Israel Institute of Technology, Haifa 32000, Israel

February 2, 2008

Abstract

The cannonball model (CB) of gamma ray bursts (GRBs) is incredibly more successful than the standard blast-wave models (SM) of GRBs, which suffer from profound inadequacies and limited predictive power. The CB model is falsifiable in its hypothesis and results. Its predictions are summarized in simple analytical expressions, derived, in fair approximations, from first principles. It provides a good description on a universal basis of the properties of long-duration GRBs and of their afterglows (AGs).

The CB model of GRBs [1,2,3,4] assumes that bipolar jets of highly relativistic CBs are launched axially in core-collapse supernova explosions (SNe). The CBs are assumed to be made of ordinary matter, as suggested by the emission of Doppler-shifted lines from the jetted CBs, ejected by the mildly relativistic μ-quasar SS 433. Crossing the SN shell (SNS) and the wind ejecta from the SN progenitor with a large Lorentz factor, the front surface of a CB is collisionally heated to keV temperatures. The quasi-thermal radiation it emits when it becomes visible, boosted and collimated by its highly relativistic motion, is a single γ-ray pulse in a GRB. The cadence of pulses reflects the chaotic accretion and is not predictable, but the individual-pulse temporal and spectral properties are predictable [2]. The GRB afterglow is mainly synchrotron radiation from the electrons that the CBs gather when they continue their voyage through the interstellar medium (ISM). It is blended with the light from the host galaxy and their smoking gun – the SNe.

Jetted CBs vs collimated fireballs. Radio, optical and X-ray observations with high spatial resolution show that μ-quasars eject relativistic plasmoids along the axis of their accretion disk when matter accretes abruptly onto their central compact object. In GRS 1915+105, the observations are

compatible with *initial* lateral expansion with a transverse velocity (in their rest system) comparable to $c/\sqrt{3}$. In XTE J1550-564 and in many quasars, such as Pictor A, the ejecta appear to travel long distances without significant lateral expansion.

In the CB model, the jetted CBs, like those observed in μ-quasars, are assumed to contain a tangled magnetic field. As they plough through the ISM, they gather and scatter its constituent protons. The re-emitted protons exert an inwards pressure on the CBs which counters their expansion. In the approximation of isotropic re-emission in the CB's rest frame and constant ISM density, n_p, one finds that within a few minutes of an observer's time, a CB reaches its asymptotic radius R. In the same approximation one may compute the

magnetic field that sustains the inwards pressure of the outgoing protons and derive an explicit law for the observed deceleration of CBs in the ISM, which depends on the initial $\gamma = \gamma_0$ as they exit the SNS, on a "deceleration" parameter x_∞ and on their viewing angle, θ, relative to their direction of motion:

$$\frac{1}{\gamma^3} - \frac{1}{\gamma_0^3} + 3\,\theta^2\,\left[\frac{1}{\gamma} - \frac{1}{\gamma_0}\right] = \frac{6\,c\,t}{(1+z)\,x_\infty}\,. \qquad (1)$$

CBs decelerate to $\gamma(t) = \gamma_0/2$ in a distance x_∞/γ_0, typically of length $\mathcal{O}(kpc)$. Eq. (1) describes well the deceleration of CBs observed in XTE J1550-564.

The original blast-wave models assumed that GRBs and their afterglows are produced by spherical fireballs. The 1997 discovery of BeppoSAX that GRBs have afterglows that appear to decline with time like a power-law was generally accepted as undisputable evidence in support of the model. However, spherical emission implies implausible energy release from small volumes. Repeated claims made by us since 1994 [5] that cosmological GRBs and their afterglows [6,7] are beamed emissions from highly relativistic jetted ejecta from stellar collapse, were olympically ignored. GRB990123 with its record "equivalent" spherical energy release in observable γ rays was the turning point of the spherical blast wave models. Fireballs became firecones [8,9] or, more properly, firetrumpets, jets of material funneled in a cone with an initial opening angle (also called θ) that increases as the ejecta encounter the ISM (see Fig. 1a). For years the modellers, unaware of the Copernican revolution, placed us, the observers, at a privileged position, precisely on-axis, so that all detected GRBs would point exactly to us. More recently, the SM view is evolving (as usual, without proper references) towards the realization that the observing angle *also* matters [10,11,12,13], a step in the

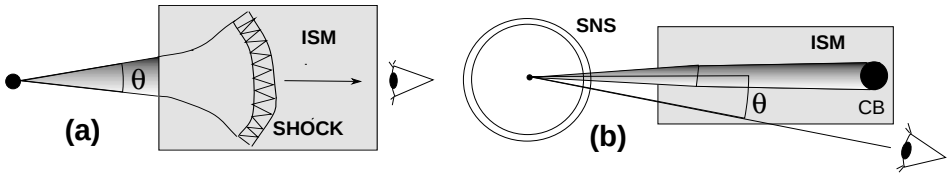

Figure 1: (a) Standard-Model geometry. (b) CB-model geometry.

right direction, advocated by the CB model [1-4]: the observation angle is the *only* one that matters.

The GRB – SN association: SNe II/Ib/Ic are far from being standard candles. But if they are not spherically symmetric –as they would be if a fair fraction of them emitted bipolar jets of cannonballs– much of their diversity can be due to the angle from which we see them. Exploiting this possibility to its extreme, i.e., using SN1998bw as an ansatz standard candle, Dar suggested [14,15] that all GRB afterglows should contain a contribution from an SN1998bw placed at the GRB position. Dar and De Rújula [1] and Dado et al. [3] have shown that the optical AG of *all* GRBs with known redshift $z < 1.12$) contain either evidence for an SN1998bw-like contribution to their optical AG (GRBs 980425, 970228, 990712 and 991208; the first and last one are shown in Fig. 2) or clear hints in the cases of GRBs 970508, 980703 and 000418 where scarcity of data, lack of spectral information and multi-colour photometry and uncertain extinction in the host galaxy prevented a firm conclusion. This suggested that most –and perhaps all– of the long-duration GRBs are associated with 1998bw-like SNe (in the more distant GRBs, the ansatz standard candle could not be seen, and it was not seen).

Naturally, "standard candles" do not exist, but taking SN1998bw as a standard candle did a good job and gave us enough confidence to *predict* how the associated SN would appear in other GRBs before they were measured. For instance, in GRB 011121 we used the first 2 days R-band data to fit the parameters describing the CBs' contribution to the AG, to predict explicitly how the AG would evolve with time, and to conclude [16] that despite the extinction in the host galaxy *"the SN will tower in all bands over the CB's declining light curve around day* ~ 30 *after burst"*. The comparison with the data [17], gathered later, is shown in Fig. 3. The SN spectrum is slightly bluer than that of 1998bw, but not significantly so. The same exercise was repeated for GRB020405. The very satisfactory results [18] are shown in Fig. 3b.

From our analysis of GRBs and their AGs we deduced that the observed

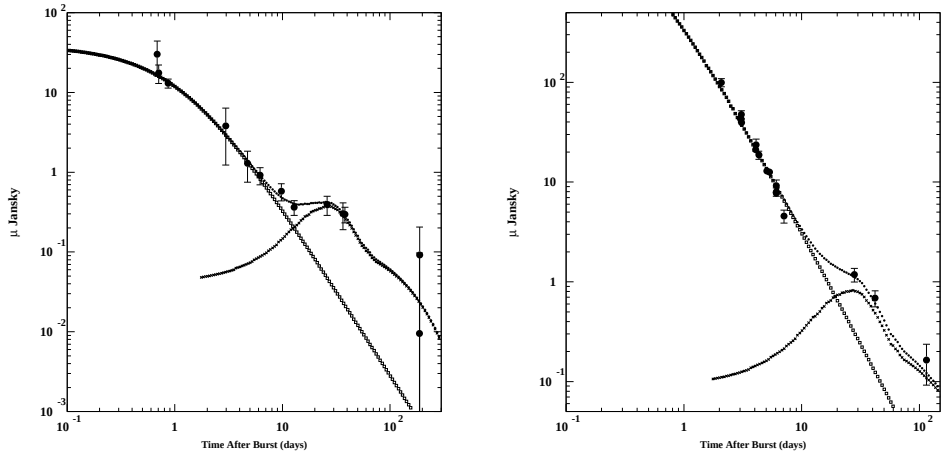

Figure 2: (a) The R-band AG of GRB970228 with the host-galaxy's contribution subtracted. (b) The R-band AG of GRB991208 with the host-galaxy's contribution subtracted.

CBs have typical Lorentz factors $\gamma \sim 10^3$ and are only observable for angles θ (between the jet axis and the observer) of $\mathcal{O}(10^{-3})$. For such a small viewing angle, the universal rate of GRBs and that of core-collapse SNe are comparable, i.e., *a good fraction of core collapse SNe emit GRBs.*

The GRB proper. During the GRB phase, the CBs are still dense and highly opaque to protons. In their rest frame, the rate of energy deposition by the incident protons near their front face is $\pi\, R^2\, n_p\, m_p\, c^3\, \gamma^2$, where R is their radius and n_p is the circumburst baryon density. Approximately, a fraction 1/3 of this energy that does not escape in neutrinos from $\pi^{\pm}$ decay, is radiated away. It is Doppler boosted and collimated by the relativistic motion of the CB, attenuated by the column density between the CB and the distant observer and redshifted by the cosmic expansion. For a typical wind profile, $n_p \sim r^{-2}$, equilibrium between energy deposition and radiation implies that an observer sees a surface radiation whose intensity per unit area is proportional to

$$I(t) \propto n_p\, e^{-\sigma_\gamma \int_r^\infty n_p\, dr'} \sim (t_m/t)^2\, e^{-2\, t_m/t}\,, \tag{2}$$

where the observer's time t and the distance r of the CB from the SN are related through $dr = \gamma\, \delta\, c\, dt/(1+z)$ and where the variation of the Lorentz

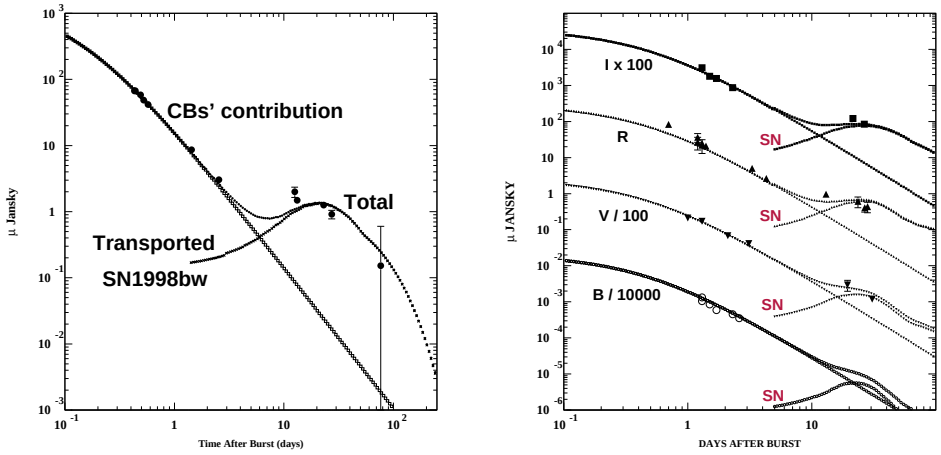

Figure 3: (a)The R-band AG of GRB011121 with the host-galaxy's contribution subtracted. (b) Broad-band optical AG of GRB020405 with the host-galaxy's contribution subtracted.

and Doppler factors of the CB, γ and δ, respectively, during the short GRB pulse were neglected. Eq. (2) has a "FRED" shape (fast rise and exponential decline) with a maximum at $t = t_m$ when the optical depth to the observer is $\tau = 2$. The photons' attenuation cross section is a sum of the bound-free (bf) and the Klein –Nishina (KN) cross sections, $\sigma_\gamma = \sigma_{bf} + \sigma_{KN}$, at photon energy $(1+z)\,E_\gamma$. Its energy dependence produces a "time lag" in $t_m \propto (1+z)/(\gamma\,\delta\,\sigma_\gamma)$, which depends moderately on energy ($\sim E^{-0.3}$) for $E_\gamma > 4/(1+z)\,keV$ (assuming a solar composition), but increases rapidly ($t_m \sim E_\gamma^{-3}$) when E_γ decreases below $\sim 4/(1+z)\,keV$. Eq. (2) can be generalized to other wind profiles.

If the energy deposition rate is balanced by a black-body-like emission, then the effective surface temperature of the CB seen by a distant observer (Doppler-shifted by a factor δ and redshifted by a factor 1+z is

$$T(t) \approx \frac{\delta}{1+z}\left[\frac{m_p\,c^2}{3\,\sigma\,\sigma_\gamma}\right]^{1/4}\left[\frac{(1+z)\,\gamma\,t_m}{t^2\,\delta}\right]^{1/4}. \qquad (3)$$

For the typical observed values $z \sim 1$, $t_{max} \sim 1\,s$ and $\gamma \approx \delta \sim 10^3$, deduced from the afterglows of GRBs with known redshift [3,4], one obtains that $T \sim 0.1\,MeV$ at maximum intensity. This explains why the typical γ-ray

energy in a GRB is [20] $\sim 250\,keV$ (for a black-body radiation, $\langle E_\gamma \rangle = 2.7\,k\,T \sim 270\,keV$). For a wind profile $n_p \sim r^{-2}$, the peak energy declines like $E_p(t) \propto T \sim t^{-1/2}$ during the pulse, where t is the time elapsed since the beginning of the pulse (not the GRB) consistent with observations (e.g., [21]). An example of γ-ray light curve, assuming a black-body emission, is given in Fig. 4a for the single pulse of GRB980425, the closest GRB of known redshift z.

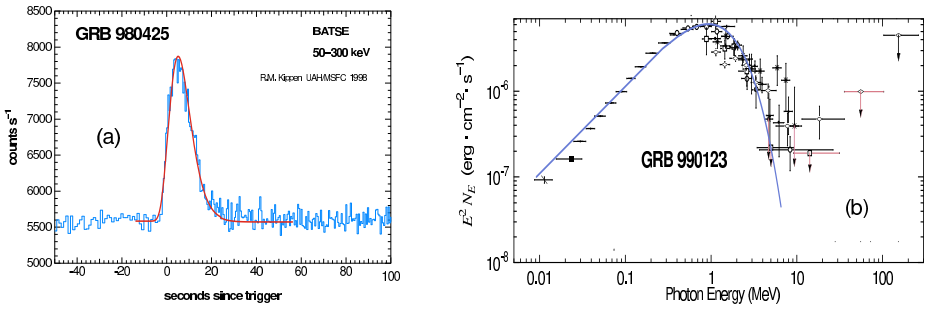

Figure 4: (a) Temporal shape of GRB980425. (b) $E^2\,dn_\gamma/dE$ spectrum of GRB990123.

An example of time-integrated black body emission is given in Fig. 4b, for the most energetic recorded GRB of known z. The low-energy part of the spectrum, in this and other GRBs [20], behaves like $E^2\,dn_\gamma/dE \sim E^1$, in agreement with the CB-model's prediction (the SM inescapably predicts a mean slope disagreeing with observation by $\sim 1/2$ unit (Ghisellini, these proceedings). The high-energy tail, however, is not well reproduced by a simplified black-body model [1]; it should be flatter. This is not surprising: the CB in its rest system is continuously bombarded by particles of high γ, which produce via Coulomb interactions a quasi-thermal distribution with a power-law tail, $dn_e/dE \sim E^{-2.2}$ instead of an exponential thermal tail. The bremsstrahlung emission from such a quasi thermal distribution of electrons from the ablated front face of the CB can be well interpolated by

$$E^2\,(dn_\gamma/dE) \approx [A\,E^{(p_1-2)s} + B\,E^{(p_2-2)s}]^{-1/s}\,, \qquad (4)$$

where $p_1 \approx 1$, $p_2 \approx 2.2$, A and B are constants whose ratio determines the peak energy and s determines the sharpness of the transition between the low energy and the high energy power-law behaviours. Indeed, the observed distributions of p_1 and p_2 (e.g. [21]) peak at these theoretical values.
Because of attenuation, only a fraction $E_\gamma^T(CB) \sim \pi\,R^2\,m_p\,c^2\,\gamma/3\,\sigma_\gamma$ of the energy deposited in the CB is observable. However, in the observer frame,

it is Doppler-boosted and relativistically collimated to a large γ-ray fluence,

$$F_\gamma[CB] = (1+z)\,\delta^3\,E_\gamma^T(CB)/(\,4\,\pi\,D_L^2) \qquad (5)$$

where D_L is the luminosity distance of the GRB and $\delta \equiv 1/\gamma\,(1-\beta\cos\theta) \simeq 2\,\gamma(t)/(1+\theta^2\gamma^2)$ in the domain of interest for GRBs: large γ and small θ. A long list of general properties of GRB pulses is reproduced in the CB-model from these formulae, that unlike the SM have a quasi-thermal origin (bremsstrahlung as opposed to synchrotron). $E_\gamma^T(CB)$ inferred from observations, behaves as a standard candle [2,22] of $\approx 10^{44}\,erg$.

GRB afterglows. Most of the observed SNe take place in super bubbles (SB) of low density. A CB exiting a SN and the presupernova wind into the low density SB, soon becomes transparent to its own enclosed radiation. At that point, it is still expanding and cooling adiabatically and by bremsstrahlung. If bremsstrahlung dominates the cooling, then the fluence of the X-ray AG decreases with time as t^{-5} . An example is shown in Fig. 5a. Many X-ray AGs are compatible with this prediction [3]. If adiabatic

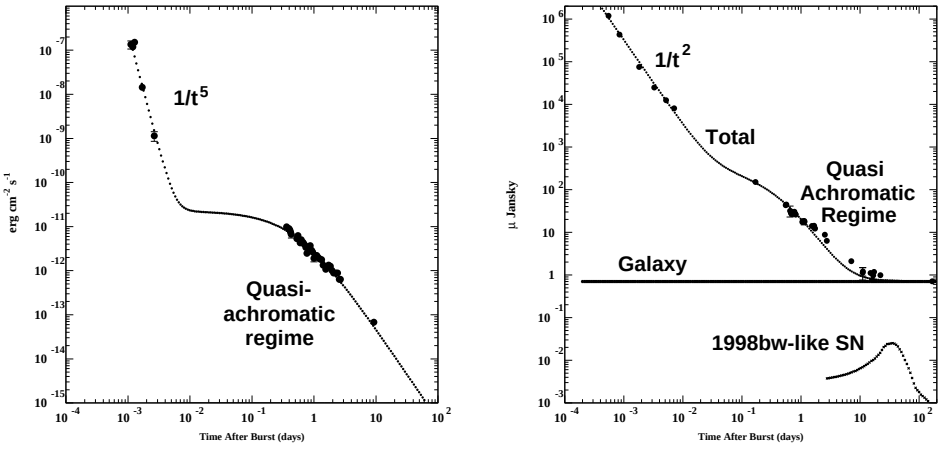

Figure 5: (a) X-ray AG of GRB010222. (b) R-band AG of GRB990123.

expansion dominates the cooling then the fluence decreases like $t^{-3.5}$. If synchrotron emission takes over while the CB still propagates in a r^{-2} density profile, its fluence decreases like t^{-2} (see Figs. 5b, 6a).

The optical AGs of *all* GRBs of known z are also well described in the CB model. They are synchrotron radiation of the electrons that the CB gathers

in its voyage through the ISM (line emission and inverse Compton scattering also contribute to the late X-ray AG). These electrons are Fermi-accelerated in the CB enclosed magnetic maze and cooled by synchrotron radiation to a broken power-law distribution with an *injection break* at the energy $E_b = m_e\, c^2\, \gamma(t)$ at which they enter the CB. The emitted synchrotron radiation has a broken power-law form [4], with a break frequency corresponding to E_b. In the observer frame, before absorption corrections, it has the approximate form:

$$F_\nu \equiv \nu\,(dn_\gamma/d\,\nu) \propto n_e\, R^2\, [\gamma(t)]^{3\alpha-1}\, [\delta(t)]^{3+\alpha}\, \nu^{-\alpha}\,, \tag{6}$$

where $\alpha \approx 0.5$ for $\nu \ll \nu_b$ and $\alpha \approx p/2 \approx 1.1$ for $\nu \gg \nu_b$, and

$$\nu_b \simeq 1.87 \times 10^3\, [\gamma(t)]^3\, \delta(t)\, [n_p/10^{-3}\ cm^{-3}]^{1/2}/(1+z)\, Hz. \tag{7}$$

is the "injection break" frequency corresponding to E_b [3]. Eq. (6) (or the interpolation formula used in [4]) describes well the observed AGs of all GRBs with known redshift [3,4,] after subtracting the contribution of the host galaxy and the SNe from the observed optical AG, and after correcting for extinction in our Galaxy and the host galaxy (which diminishes with time as the CB moves far away from the explosion site). This is demonstrated in Figs. 2, 3, 5, and 6.

Temporal breaks. In the CB model, changes in the temporal decline rate of the AG of a CB have two distinct origins: the deceleration of the CB and changes in the ISM density along its trajectory:

Eq. (1) implies that $\gamma(t)$ and consequently also $F_\nu(t)$, change very little when $t < t_0\,(1+3\,\gamma_0^2\,\theta^2)$, where $t_0 = (1+z)\,x_\infty/6c\,\gamma_0^3$. Later, when $t \gg t_0\,(1+3\,\gamma_0^2\,\theta^2)$ and $\gamma^2\,\theta^2 \ll 1$, $\gamma(t)$ approaches its asymptotic $\sim t^{-1/3}$ behaviour and $F_\nu(t) \sim t^{-(4\alpha+2)/3} \sim t^{-2.13}$ if $\nu \gg \nu_b$ and $\sim t^{-1.33}$ if $\nu \ll \nu_b$. The transition of $F_\nu(t)$ around $t = t_0\,(1+3\,\theta^2\,\gamma_0^2)$ to its asymptotic behaviour is achromatic and gradual.

Eq. (6) implies that a chromatic break in the AG takes place when $\nu_b(t)$ crosses the observed band at time $t = t_b$, where $\nu_b(t_b) = \nu$. If $F_\nu(t) \sim t^{-\beta}$ before the break, then $F_\nu(t) \sim t^{-1.6\beta}$ right after it.

Eqs. (1),(6) also imply that variations in the ISM density induce corresponding variations in $F_\nu(t)$ and $\nu_b(t)$, which are proportional to n_p and $\sqrt{n_p}$, respectively.

All these possibilities have materialized, e.g. in the AG of GRB021004, [22] as shown in Fig. 7a. Moreover, since the CB model successfully describes all the observed AGs of GRBs with known redshift, it does explain also the so-called "breaks" in these AGs, when they are there. The firetrumpet

models have claimed to produce sharp breaks in the AGs when the beaming angle becomes larger than the opening angle of the ejecta [8.9]. However, they are not reproduced by detailed calculations that properly take into account arrival time and viewing angle effects. Thus, also the "standard candle energy", derived in the SM [23] [by extracting opening angles from temporal "breaks" in AGs, is baseless! Both the temporal and spectral

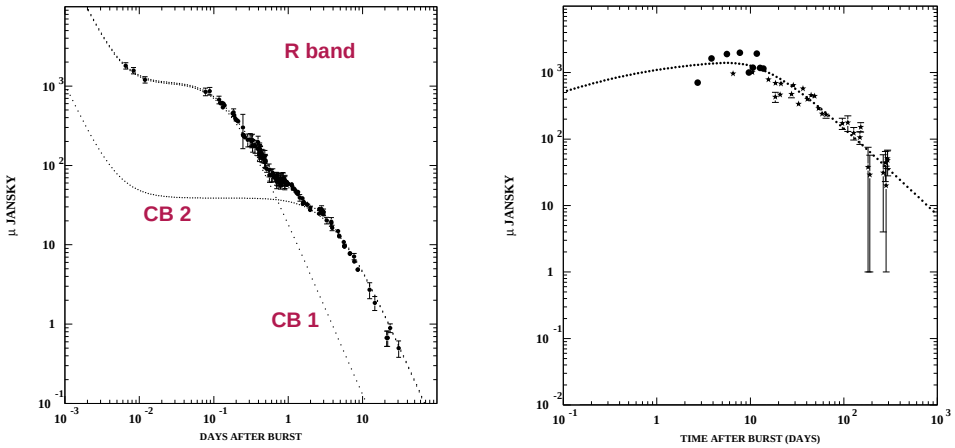

Figure 6: (a) The predicted host-galaxy-subtracted R-band light of GRB021004 from a 2 CB broad-band fit to its AG []. (b) The 8.46 GHz radio light curve of GRB991208 and that obtained from the CB model fit to its broad-band AG

evolution of optical AGs are well reproduced by the CB model. In particular, the predicted value, $p \approx 2.2$, is in agreement with all the data on X-ray AGs and on relatively late-time optical AGs, where $\nu \gg \nu_b$ and $F_\nu \propto \nu^{-\alpha}$ with $\alpha = p/2 \approx 1.1$ (after correcting for Galactic extinction).

Broad-band spectra. In the radio domain, self-absorption in the CB is important. The dominant mechanism is free–free attenuation, characterized by a single parameter ν_a in the opacity, which behaves as $\tau_\nu = (\nu_a/\nu)^2 \, (\gamma(t)/\gamma_0)^2$. Absorption in the CB produces a turn-around of the spectra from $F_\nu \sim \nu^{1.5}$ to $F_\nu \sim \nu^{-0.5}$ behaviour. The complete description of the radio AG requires the inclusion of two additional effects that, in fair approximations, introduce no extra parameters: a "cumulation factor" for the electrons that emit the observed radio frequencies (it takes time for the ISM electrons gathered by the CB to cool to radio-emitting energies)

and an "illumination and limb-darkening" factor taking into account that the CBs are viewed relativistically (an observer would "see" almost all of the 4π surface of a spherical CB). With these corrections to Eq. (6), the measured broad-band AG of all GRBs with known z are well fitted, in spite of the scintillations in the radio. The overall successful fits [4] involve only one additional "radio" parameter, ν_a. The most complete broad-band data are perhaps those of GRB991208. Fig. 7b compares its measured radio light-curve at 8.46 GHz and the CB model light-curve, obtained from the broad-band fit. A comparison between its observed and predicted spectrum between 5 and 10 days after burst is shown in Fig. 7a.

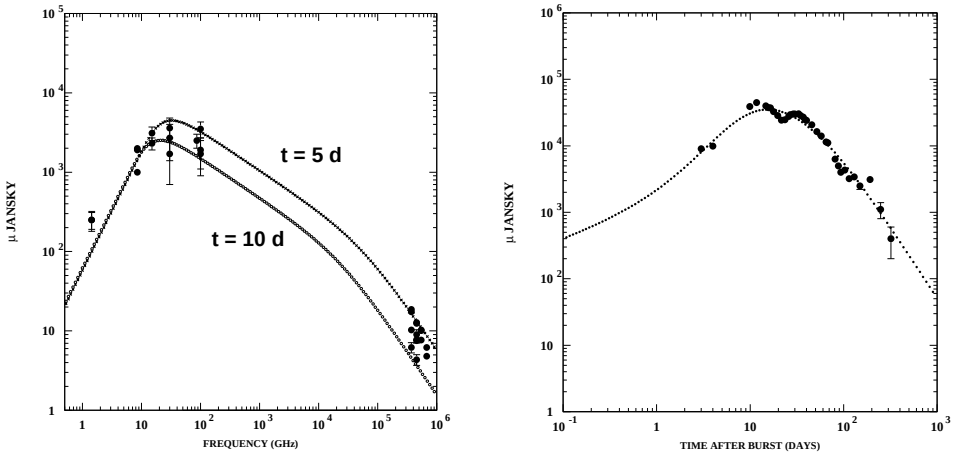

Figure 7: (a) The CB-model fit to the broad-band spectrum of GRB991208 at $t = 5$ to 10 days. (b) 4.8 GHz light curve of GRB980425. At other times and frequencies the fits are equally good.

GRB980425/SN1998bw. In the CB model, this GRB and its associated SN1998bw are **not** exceptional. Because it was viewed at an exceptionally large angle, $\sim$ 8 mrad, its γ-ray fluence was comparable to that of more distant GRBs, viewed at $\theta \sim 1$ mrad [1,3]. That is why its optical AG was dominated by the SN, except perhaps for the last measured point. The X-ray AG of its single CB (see Fig. 8a) is of "normal" magnitude, it is *not* emitted by the SN. Its predicted late-time behaviour [3] is consistent with the Chandra and XMM-Newton measurements reported in this meeting by Kouveliotou and Pian. The normalization, spectral and temporal behaviour of the radio AG of this GRB are also "normal" and due to the CB, **not** the

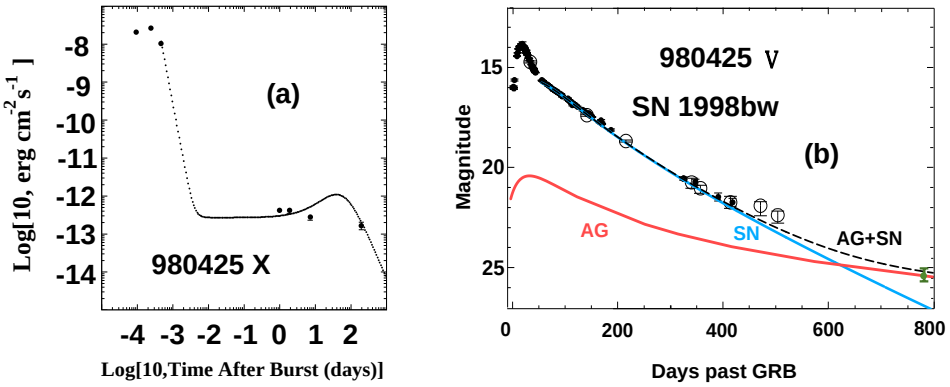

Figure 8: CB-model fits to GRB 980425. (a) The X-ray AG. (b) The V-band AG: the SN contribution, the CB's contribution and the total. All parameters (but z and θ) are "normal".

SN [3]. The predicted radio light-curve at 4.8 GHz of GRB980425 and the data are shown in Fig. 7b. SN1998bw, deprived of its "abnormal" X-ray and radio emissions (which it did not emit!), loses most of its "peculiarity".

Radio scintillations of pulsars have been used to measure their sky-projected velocities, in agreement with proper-motion measurements. For cosmological GRBs, the sky angular velocity of their CBs happens to be comparable to that of the much slower and closer Galactic pulsars. Perhaps, then, the analysis of GRB radio oscillations may result in a measurement of their apparent "hyperluminal" velocities [4].

X-ray lines observed in the AG of some GRBs, if real, may be Balmer and Lyman lines from hydrogen recombination in the CBs, Doppler-boosted by their highly relativistic motion and redshifted by the cosmic expansion. Then, these lines should be narrow and their observed energy, $E(t) = \delta(t)\, E_{line}/(1+z)$, where E_{line} is their energy in the CB rest frame, should move with time to lower energy as the CBs decelerate and their Doppler factor diminishes with time. Current data are not precise enough to distinguish between metal lines from photoionized circumburst matter and the CB model interpretation, but the time-dependence of these lines may be observable [24].

For lack of time and space I could not discuss the CB model interpretation of *dark bursts, short GRBs and X-ray Flashes* that will be published elsewhere.

Concluding remarks The CB model is very modest in the adjectives

that refer to GRBs. None of them is exceptional, not even the very energetic GRB 990123, nor 970508 with its peculiar AG shape, nor the extraordinarily close-by 980425. They are all associated with asymmetric supernovae seen from near their axis and visible when they are not too far or too extinct. The explosions that generate GRBs are neither "the biggest after the Big Bang" nor "hypernovae". The mechanism that begets GRBs is common: it takes place in quasars as well as microquasars. The model works very well and is very predictive, thus falsifiable.

acknowledgements The author would like to thank the conference organizers Franco Giovannelli and Giampaolo Mannocchi for the invitation, the theory division of CERN for its hospitality and the VPR fund for promotion of research at the Technion for its support.

References

[1] A. Dar and A. De Rújula, astro-ph/0008474 (2000)

[2] A. Dar and A. De Rújula, astro-ph/0012227 (2000)

[3] S. Dado, A. Dar and A. De Rújula, A&A, 388 (2002) 1079

[4] S. Dado, A. Dar and A. De Rújula, A&A in press (astro-ph/0204474)

[5] N.J. Shaviv and A. Dar, ApJ 447 (1995) 863

[6] A. Dar, astro-ph/9704187 (1997)

[7] A. Dar, ApJ 500 (1998) L93

[8] J.E. Rhoads, ApJ 525 (1999) 737

[9] R. Sari, T. Piran and J. Halpern, ApJ 519 (1999) L17

[10] E. Rossi, D. Lazzati and M.J. Rees, MNRAS 332 (2002) 945

[11] B. Zhang and P.L. Meszaros, ApJ 571 (2002) 876

[12] J.D. Salmonson and T.J. Galama, ApJ 569 (2002) 682

[13] J. Granot, A. Panaitescu, A. Kumar and S.W. Woosley, ApJ 570 (2002) 61

[14] A. Dar, 1999a, A&A 138S (1999) 505

[15] A. Dar, GCN Circ. 346 (1999)

[16] S. Dado, A. Dar and A. De Rújula, ApJ (2002) L143

[17] J.S. Bloom, et al. ApJ 572 (2002) 45L

[18] S. Dado, A. Dar and A. De Rújula, A&A 393 (2002) L25

[19] R.D. Preece, et al. 2000, ApJS, 126 (2000) 19

[20] L.A. Ford, et al. 1995, ApJ, 439, 307

[21] R. Plaga, 2001, A&A 370 (2001) 351

[22] S. Dado, A. Dar and A. De Rújula, ApJ, in press (astro-ph/0211224)

[23] D.A. Frail, et al. 2001, ApJ, 562, L55

[24] S. Dado, A. Dar and A. De Rújula, ApJ in press (astro-ph/0207015)